Effect of Substrate Geometry on Polymer Molecular Weight and Polydispersity during Surface-Initiated Polymerization

Christopher B. Gorman,*,† Randall J. Petrie,†,§ and Jan Genzer*,‡

Department of Chemistry, North Carolina State University, Raleigh, North Carolina 27695-5079, and Departments of Chemical & Biomolecular Engineering, North Carolina State University, Raleigh, North Carolina 27695-7905

Received March 4, 2008; Revised Manuscript Received April 24, 2008

ABSTRACT: Poly(methyl methacrylate) (PMMA) anchored chains were grown on porous silicon (p-Si) and anodically etched aluminum oxide (AAO) substrates via surface-initiated atom transfer radical polymerization (ATRP). Using hydrogen fluoride, the chains could be cleaved from the substrates, as evidenced by infrared spectroscopy. The molecular weights and molecular weight distributions of PMMA could be analyzed directly on these substrates (after cleaving the chains from the support) using direct ionization mass spectrometry (DIOS-MS) and matrix-assisted laser desorption ionization mass spectrometry (MALDI-MS). Two principal conclusions were drawn from the study. First, matrix-free DIOS-MS was effective at direct analysis of the polymers up to a molecular weight of ≈6 kDa; the signal-to-noise ratio for heavier polymer chains diminished rapidly. Second, under the same polymerization conditions, PMMA grown on both p-Si and AAO substrates had a much lower molecular weight and a broader molecular weight distribution than that grown in solution. Confinement effects imposed by the pores during the polymerization are proposed as the likely mechanism for the reduced growth rates and more polydisperse chains.

Introduction

Surface-grafted polymer assemblies facilitate tunability of chemico-physical properties of surfaces, thus making them amiable for a variety of applications, including controlling colloidal dispersions, tailoring protein adsorption, generating responsive surfaces, and fabricating chemical gates.[1] Polymer brushes can be formed via two methodologies. In the so-called "grafting onto" method, polymers are synthesized ex situ and subsequently chemically grafted onto the substrate. While simple to carry out, this method usually produces polymer brushes with low polymer grafting densities. Higher chain grafting density can be attained via the so-called "grafting from" methodology, which is based on decorating the material surfaces with polymerization initiators and performing the polymerization directly on the surface. The "grafting from" method was successfully used to form homogeneous layers of surface-anchored homopolymers and block copolymers[2–4] as well as structures comprising patterned assemblies of homopolymers[5–12] and copolymers.[13] One of the major drawbacks of the "grafting from" approach is that that structure of the polymer may be profoundly influenced by confinement effects imposed by the substrate.[14] Different applications require that polymer brushes be prepared on various substrate geometries, including flat, convex, and concave surfaces. Depending on the geometry, the growing chains will experience different degrees of confinement that may ultimately affect the chain molecular weight and molecular weight distribution.[14] While confinement effects are not severe for small spheres, when polymer brushes are grown on flat or concave surfaces strong spatial restrictions exist.

Despite the relatively large body of experimental work on "grafting from" polymerization, our understanding of confinement effects on the characteristics of polymer brushes is still limited. To date, most systems studied have involved polymer brushes on convex surfaces, such as nano/micro-sized spheres.[15–20] The molecular weight and polydispersity index (PDI), measured with size exclusion chromatography (SEC) on polymers cleaved from the spheres after the polymerization, were found to be close to the values obtained from analogous polymerizations in solution. While polymer brushes have also been grown inside concave substrates, such as porous silica,[21] the intergallery regions of silicates (clays),[22–26] and silica capillaries,[27–29] limited information exists about the molecular weight and PDI of these samples. Literature data on the properties of polymer brushes grown on flat substrates are in most cases restricted to reporting how the thickness of the brush layer varies with the initiator structure,[30] initiator grafting density,[31,32] and polymerization conditions,[33] although a few studies reported also on molecular weight and PDI.[13,33]

The purpose of this paper is twofold. First, the effect of confinement imposed by concave geometry on surface-initiated polymerization is explored by studying two types of concave substrates with different dimensions: porous silicon (p-Si) and anodic aluminum oxide (AAO) with pore sizes of ≈50 and ≈200 nm, respectively. Atom transfer radical polymerization (ATRP), pioneered by Sawamoto[34] and Matyjaszewski,[35] is used because of its ability to synthesize functionalized polymers with well-defined composition, structure, and a reasonably small polydispersity index, relative to the free radical process.[36,37] The second objective is to explore whether the p-Si support can be employed to study the molecular weight distribution of polymers by utilizing desorption ionization on silicon mass spectrometry (DIOS-MS), a variant of an established technique called matrix-assisted laser desorption ionization (MALDI-MS). DIOS-MS has the added advantage of eliminating the extra signal associated with the organic matrix normally used to analyze synthetic polymers using MALDI-MS.[38–41] Thus, if low molecular weight fractions of the polymer existed on the surface, such as those resulting from restricted growth as the result of the aforementioned confinement effects, their presence would not be obscured by the matrix.

Materials and Methods

Preparation of Porous Silicon. The porous silicon (p-Si) substrate was created by electrochemical etching an n-type silicon

* Corresponding authors. E-mail: Chris_Gorman@ncsu.edu, Jan_Genzer@ncsu.edu.
† Department of Chemistry.
‡ Departments of Chemical & Biomolecular Engineering.
§ Present address: BASF Corporation, Charlotte, NC.

10.1021/ma8004857 CCC: $40.75
Published on Web 06/10/2008

wafer (Sb-doped, 0.01−0.02 ohm·cm, Silicon Valley Microelectronics) in a Teflon cell with a configuration similar to the cell used by Siuzdak et al.[42] The etching solution was a 1:1 (by volume) mixture of concentrated HF (49% Reagent Grade, Fisher) and absolute ethanol (100%, Fisher). The cell compartment that contained the silicon wafer and the etching solution was illuminated with 50 mW/cm^2 of white light from a fiber-optic light source (Model I-150, Coherent, Inc.). While illuminated, ≈4.6 mA/cm^2 of constant current passed through the cell chamber for 1 min. After the etching process, the p-Si sample was washed with absolute ethanol and dried under a nitrogen stream. Following the original etch, a 1 min "postetch" was performed using a 10% aqueous solution of HF for 1 min. After the "postetch" process, the p-Si sample was washed with absolute ethanol and dried under a nitrogen stream. The sample was immersed in absolute ethanol until used.

Initiator Attachment to Concave Substrates. (11-(2-Bromo-2-methyl)propionyloxy)undecyltrichlorosilane (BMPUS) was prepared according to the procedure of Matyjaszewski and co-workers.[2] The p-Si substrate was exposed to ultraviolet/ozone cleaning (UVO) prior to initiator attachment. The AAO membrane (0.2 μm, Whatman) was ultraviolet/ozone (UVO) cleaned for 20 min on each side. An aliquot of 20 μL of 5% BMPUS in anhydrous toluene was added to cold anhydrous toluene (20 mL, 99.8%, Sigma-Aldrich) containing either the p-Si or AAO substrate and placed in the freezer (≈−15 °C) for at least 12 h. The substrates were then rinsed with toluene (Reagent grade) and allowed to dry under a gentle stream of nitrogen.

Surface-Initiated Polymerization of Methyl Methacrylate. A room-temperature-based aqueous/solvent-based atom transfer radical polymerization (ATRP) system discussed earlier was chosen for the polymerization of methyl methacrylate; the setup closely followed the work done by Huck and Jones.[43] The use of this system produced a homogeneous solution that kept the growing polymer chains solvated throughout the entire reaction time. A single homogeneous solution containing all the components needed for the ATRP polymerization of PMMA was prepared and consisted of 34.9 g of methyl methacrylate (MMA, 99%, Alfa Aesar), 32.2 g of methanol (Reagent Grade), and 7 g of DI water. The polymerization system also contained 0.64 g of Cu(I)Cl (99%, Aldrich) catalyst and 0.011 g of Cu(II)Cl_2 (99%, Aldrich) inhibitor. In addition, 2.06 g of 2,2′-dipyridyl (99%, Aldrich) was added as a ligand to complex with the copper compounds and keep the whole system homogenous. The solution was prepared under a constant nitrogen stream in a 200 mL two-neck round bottom flask to keep oxygen from penetrating the system.

Bulk polymerization of MMA was performed by filling 20 mL vials with polymerization media and adding 1 μL of ethyl 2-bromoisobutyrate (98%, Aldrich), which acted as an initiator. The vials were tightly sealed, and nitrogen was bubbled through the solution during the polymerization. The polymerizations times ranged from 30 to 130 min. At the end of each respective polymerization time, the polymerization solution was poured into a 200 mL jar and filled with methanol (Reagent Grade, Aldrich) to precipitate the solution-grown polymer. The methanol/polymer medium was exposed to oxygen for 30 min, which ensured that all the CuCl has been oxidized to $CuCl_2$ and the polymerization has been effectively stopped. The precipitated PMMA was then placed in the freezer and allowed to settle, after which it was decanted and dissolved in chloroform. The polymer was then run through several (2−3) pipets filled with activated alumina to remove the $CuCl_2$. Chloroform was used to elute the PMMA.

PMMA brushes on p-Si and AAO were formed by filling polymerization solution into 20 mL vials that contained either a single p-Si wafer functionalized with the BMPUS initiator of an AAO substrates decorated with BMPUS. The vials were tightly sealed and nitrogen was bubbled through the solution during the polymerization. The polymerizations were carried out for various times ranging from 30 min to 3 h. At the end of each respective time, the polymerization solution was removed and discarded, and the porous silicon wafer was rinsed with methanol and blown-dry with a nitrogen stream.

PMMA Cleavage from the Substrate. The PMMA-modified p-Si was placed in Petri dish along with 2−3 mL of 10% solution of HF acid (49% Reagent Grade, Fisher) that was contained in a smaller Petri dish. The HF vapors were allowed to react with Si−O bonds for 40 min. A transmission infrared spectrum was taken of the p-Si substrate following this step as shown in Figure 4. For the infrared spectroscopy experiment the PMMA cleaved p-Si substrate was washed with methylene chloride (HPLC Grade, Sigma-Aldrich). A transmission infrared spectrum was taken of the p-Si substrate following this step as shown in Figure 4.

The PMMA-modified AAO membranes were removed from the vial and washed with copious amounts of methanol. A transmission infrared spectrum was taken of the AAO membrane following this step as discussed in the text. The PMMA modified AAO membranes were then placed in a 200 mL plastic container and a 10% aqueous HF (49% Reagent Grade, Fisher) solution was added. The sample was allowed to sit for a minimum of 30 min. Then, 10 mL of chloroform was added and stirred to capture the PMMA chains in the organic phase. The chloroform was extracted with a syringe and placed in a small vial (5 mL).

Mass Spectrometry. An Applied Biosystems Voyager STR MALDI-TOF mass spectrometer was used for the molecular weight analysis. It was operated at an accelerating voltage of 20 kV in linear mode and positive ions were collected; grid voltage was 90%. Laser intensity was adjusted to optimize signal. Generally, laser intensity between 1800 and 1900 proved sufficient. All settings are specific to the Applied Biosystems Voyager STR MALDI-TOF mass spectrometer.

DIOS-MS Analysis of PMMA Grown in p-Si. Aliquots of THF (3−5 5 μL) were dropped onto the surface of the cleaved PMMA modified p-Si in order to draw the polymer out of the pores to the surface for easier ablation. Sodium trifluoroacetate (NaTFA 98%, Sigma-Aldrich) was used to charge the polymer. The sodium trifluoroacetate solution was prepared for concentrations ranging from 0.5 to 5 mg/mL (in THF). Aliquots of the sodium trifluoroacetate (2−3 × 3 μL) were added to the surface of the porous silicon at different positions of the porous silicon substrate to facilitate detection in the MALDI-MS.

MALDI-MS Analysis of PMMA Grown in AAO and Bulk. The chloroform/PMMA solution was prepared in a small 5 mL vial. A 0.1 M solution (in THF) of α-cyanohydroxycinnamic acid (99%, Sigma-Aldrich) was prepared in a 1 mL centrifuge tube. The PMMA was then mixed in a specific ratio. The ratio used varied from 3−5 to 1 (by volume) of α-cyanohydroxycinnamic to PMMA.

Size Exclusion Chromatography (SEC). PMMA polymers were dissolved in chloroform (HPLC grade, Aldrich) and filtered through glass microfiber filters (0.45 μm pore size, Whatman). Samples were placed in 1 mL SEC vials and loaded into the autosampler with a bulk flow rate of 0.3 mL/min. Each autoinjection was 100 μL. Three Waters Styragel HR columns were used in series: 500−500 000 Da for column one, 50−100 000 Da for column two, and 500−30 000 Da for column three. A Wyatt Optilab Rex differential refractometer was the concentration detector, and the unknown samples were compared to PMMA standards ($\bar{M}_n$ = 1.8, 3.25, 6.8, and 12.3 kDa).

Fourier Transform Infrared (FTIR) Spectroscopy. FTIR spectroscopy was collected in the transmission mode with Nicolet 750. A total of 1024 scans were made with resolution 4 cm^{-1} for each measurements, which required a scanning time of ≈12 min. The IR spectra for polymer bulk were measured with the KBr pellets. Samples with polymers attached on the substrate were scanned directly though the wafer; a bare silicon wafer was used as the blank. The IR spectra were analyzed using the OMNIC 5.0 software.

Results

MALDI-MS and DIOS-MS on Standard PMMA Samples. Over the past few years, MALDI-MS has become a routine analytical tool for determining molecular weight distribution of oligomers and polymers.[44] The primary attribute

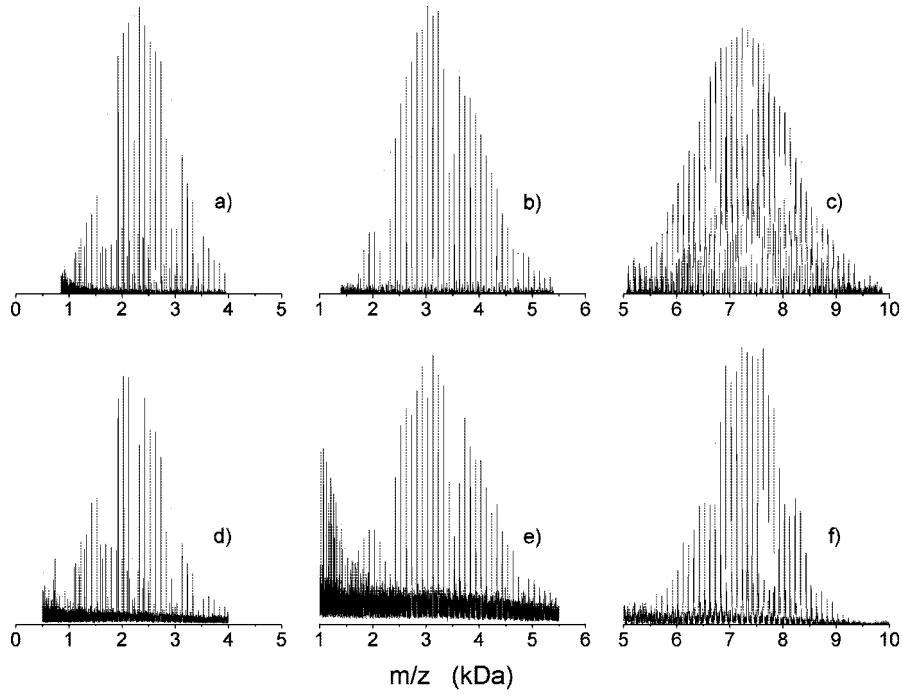

Figure 1. MALDI-MS spectra (top row) and DIOS-MS spectra (bottom row) collected from four PMMA standard samples with nominal number-average molecular weights of 1.8 (a, d), 3.25 (b, e), and 6.4 kDa (c, f), as specified by the manufacturer (Polymer Standards Service, Inc.).

of MALDI-MS is the ability to measure molecular weight distributions directly without using any standards. While the upper limit of the molecular weight to be determined is several tens of kDa, a value that is constantly increasing with as the technique is further developed, there exists also a lower limit to the molecular weight of analytes that can be measured by MALDI-MS. Specifically, as the molecular weight of the oligomers approaches that of the matrix, it becomes increasingly difficult to accurately deconvolute the mass spectrum collected from the analyte from that originating from the matrix material. In recent years, desorption ionization on silicon mass spectrometry (DIOS-MS) has emerged as a technique that potentially minimizes this problem. Because DIOS-MS does not require any matrix, polymers with much smaller molecular weight can potentially be analyzed. DIOS-MS utilizes laser light to initiate desorption of analyte molecules from the surface without matrix assistance; a typical substrate used in such studies is porous silicon (p-Si). In addition to facilitating the energy transfer from the laser pulse to the analyte, the concave geometry of p-Si offers a larger surface area relative to flat substrates.[42,45] As will be shown later in the paper, the concave geometry of p-Si substrates is conveniently suited to study the effect of confinement on surface-initiated polymerization and concurrently capitalize on the fact that the polymer brushes grown inside silicon pores can be analyzed with DIOS-MS.

First, it was established that DIOS-MS is indeed capable of accurately monitoring the molecular weight of polymers. In order to test this notion, samples of monodisperse poly(methyl methacrylate) (PMMA) standards (Polymer Standards Service), whose nominal molecular weights ranged from $\approx$2 to $\approx$24 kDa, were analyzed. Figure 1 shows the MALDI-MS spectra from PMMA having (a) 1.8, (b) 3.25, and (c) 6.4 kDa, as specified by the manufacturer. These spectra were obtained by using 0.1 M α-cyanohydroxycinnamic acid as the matrix in a 5 to 1 ratio of matrix to PMMA standard (0.1 mM). The signal-to-noise ratio deteriorated once the molecular weight exceeded 15 kDa. Concurrently, DIOS-MS analysis of the same set of PMMA standards was performed. Figure 1d−f shows the DIOS-MS spectra from the same specimens as shown in Figure 1a−c. Collection of spectra for the 1.8 and 3.25 kDa standards was accomplished with little effort to optimize the analysis conditions. However, in comparing these standards, the spectra of the two lower molecular weight PMMA standards exhibited a higher signal-to-noise ratio and yielded higher counts (corresponding to the number of ions collected) than that of the 6.4 kDa sample. Attempts to collect a spectrum of the $\geq$6.4 kDa PMMA standards proved more difficult. In many cases the spectrum collected from specimens having higher molecular weights exhibited less than a 2 to 1 signal-to-noise ratio. After adjusting the accelerating voltage to optimize the signal, a spectrum with better than 2 to 1 signal-to-noise was recorded. The number of counts also decreased significantly for those samples but still gave a molecular weight distribution expected for these standards. While, in general, the DIOS-MS spectra had a comparable signal-to-noise ratio to those measured by MALDI-MS with the conventional matrix added, the intensity of signal corresponding to the number of ion counts decreased more rapidly with DIOS-MS as the molecular weight of the sample increased. This result suggests that the ablation of higher molecular weight species is less efficient in DIOS-MS as compared to the conventional MALDI-MS technique.

The weight-average molecular weight ($\bar{M}_w$), number-average molecular weight ($\bar{M}_n$), and polydispersity index (PDI) were calculated using a two-parameter Schultz distribution fit,[46,47] which is designed to model the most probable fit for the molecular weight distribution. A "point-by-point" fit was also performed yielding results to compare to the Schultz distribution fit. Unlike the Schultz distribution fits, which models the Gaussian curve of the polymers distribution, the point-by-point fit simply takes the local maxima of all the individual monomer units along with the relative intensities to find the $\bar{M}_w$, $\bar{M}_n$, and PDI. (See the Appendix for a complete description of the Schultz and point-by-point fit.) The results of the Schultz and point-by-point distribution fits are shown in Figure 2 by closed and open symbols, respectively, for both MALDI-MS (squares) and DIOS-MS (circles) analysis. Generally, both techniques provide comparable results for molecular weight distributions of PMMA standards.

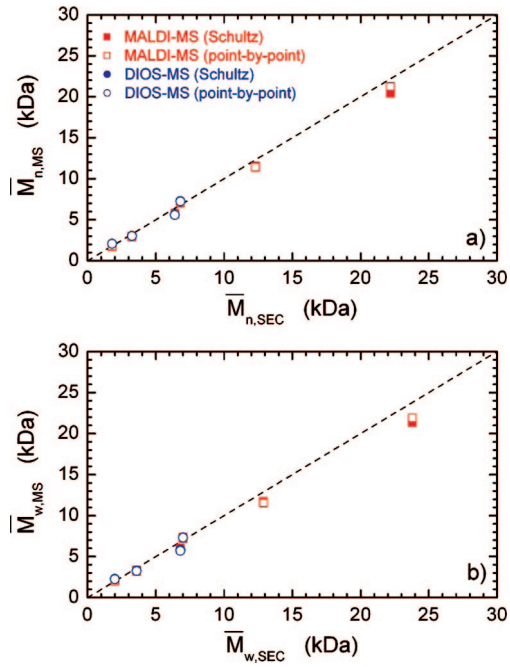

Figure 2. (a) Number-average and (b) weight-average molecular weight from PMMA standard samples (Polymer Standards Service, Inc.) determined by MALDI-MS (squares) and DIOS-MS (circles) plotted against the respective molecular weight obtained from SEC experiments. The solid and open symbols denote the values determined by fitting to a Schultz distribution and obtained by a point-by-point calculation method, respectively.

Formation of PMMA Brushes Inside p-Si Substrate and Analysis of Molecular Weight Distribution. The comparison of MALDI-MS and DIOS-MS analysis of PMMA standards indicated that DIOS-MS should be readily capable of evaluating the molecular weight distribution of polymers having molecular weights on the order or a few kDa. As one of the chief objectives of this work was to investigate the effect of concave confinement on "grafting-from" polymerization, porous silicon (p-Si) was explored as a platform for generating such a concave confinement. These p-Si substrates were produced as described in the Materials and Methods section using the standard "double etching" method of flat silicon wafers. The pore size in thus prepared substrates was ≈50 nm, as determined from scanning electron microscopy (Figure 3). Ultraviolet/ozone (UVO) treatment was employed to produce a thin silica layer inside the pores of the p-Si support. The hydroxyl functionalities present on top of this silica layer served as attachments points for (11-(2-bromo-2-methyl)propionyloxy)undecyltrichlorosilane (BMPUS), which acted as the polymerization initiator. The polymerization of MMA was conducted using the methodology described in the Materials and Methods section. After polymerization, the polymers were cleaved from the substrate by exposing the specimens to HF vapor, which effectively eliminated the silica layer while leaving the polymers inside the pores. Figure 3 depicts schematically the aforementioned steps. Figure 4 shows infrared (IR) spectra collected after each individual step. After attachment of the BMPUS initiator to the surface of the porous silicon wafer (n-type, Sb-doped, 0.01−0.02 ohm·cm, Silicon Valley Microelectronics, Inc.), a carbonyl stretch appeared at ≈1732 cm^{-1} (e.g. the black line marked 3 in Figure 4). This feature was not observed prior to treatment of the porous silicon with BMPUS. The polymer brush was then grown using the "grafting from" ATRP technique described earlier. The main characteristic for the presence of surface-bound PMMA is the slight shift and an increase in the relative intensity of the carbonyl stretch at ≈1738 cm^{-1} (e.g., the red line marked 4 in Figure 4). As expected, after polymerization, the carbonyl stretch intensity increases because of the increased number of C═O bonds that are in each repeat unit of the polymer. Etching the sample with HF vapor resulted in the disappearance of the Si−O signal as demonstrated by the green line marked 5 in Figure 4. In order to confirm the polymer cleavage, the sample was extracted with methylene chloride to remove any physisorbed PMMA polymer. The disappearance of the carbonyl stretch after this procedure indicated that the polymer could be removed in this manner. After the methylene chloride extraction, the loss of the carbonyl stretch at 1738 cm^{-1} can be observed (e.g., the blue line in Figure 4). This set of experiments thus demonstrates that both polymerization of PMMA and its cleavage from p-Si are feasible.

DIOS-MS analysis was carried out on several different samples in which the polymerization time was varied. Figure 5 depicts representative data of the molecular weight distribution of PMMA grown for 3 h that was directly measured from the surface of porous silicon after cleaving the polymer with HF vapor using the procedure described earlier. The spectrum exhibits two groups of peaks separated by the mass of the repeat unit (100.1 Da). Each of these groups presumably differs by the size of the group that has terminated those polymer chains. We refer to those two distributions as *09 and *65 and provide further insight into the chemical structure of the cleaved chains in the Discussion section. A detailed analysis of the spectrum using the point-by-point method (see Appendix for details) computes $\bar{M}_w \approx 1050$ Da and $\bar{M}_n \approx 880$ Da. No attempts were made to fit the distribution to the Schultz model as the shape of the distribution seemed to follow the expected functional form of the normal distribution. Despite varying the polymerization time, the molecular weight of the PMMA measured was never found to be above ≈2 kDa. A more quantitative comparison of PMMA grown inside p-Si and PMMA prepared from polymerization in solution will be given in the Discussion section.

Formation of PMMA Brushes Inside AAO Substrates and Analysis of Their Molecular Weight Distribution. While polymerization inside p-Si substrates clearly produced PMMA brushes, their molecular weight was very low relative to the bulk polymerization. Furthermore, measurement of molecular weights of ≈6 kDa from direct MS on p-Si (Figure 1) suggested that this low molecular weight was not an artifact of the MS measurement. Thus, the low molecular weights measured were attributed to the confinement effect experienced by the growing PMMA chains inside very small concave spaces. In addition, because of the nature of the etching process, the pore distribution inside p-Si substrate was not very uniform. In order to investigate polymerization in concave spaces further, polymerization in anodic aluminum oxide (AAO) membranes was studied. While AAO membranes have primarily been used as nano/micron pore sized filters, recent studies demonstrate new applications of AAO as templates for nanomanufacturing.[48] It was anticipated that PMMA grown inside the larger pores in AAO (≈200 nm) relative to p-Si (≈50 nm) should have a higher molecular weight. Furthermore, it was anticipated that the process should be more controlled as the larger and more uniform pores in AAO should facilitate a better controlled transport of monomer and the catalyst needed for controlled polymerization.

FTIR was used to monitor the steps involved in preparing PMMA brushes inside the AAO membrane. The top spectrum in Figure 6 depicts the signal collected from BMPUS-modified AAO substrates. The main feature in this spectrum is the appearance of a carbonyl stretch at ≈1738 cm^{-1}, not observed prior to the initiator attachment to the AAO membrane. The polymer brush was then grown using the "grafting from" ATRP

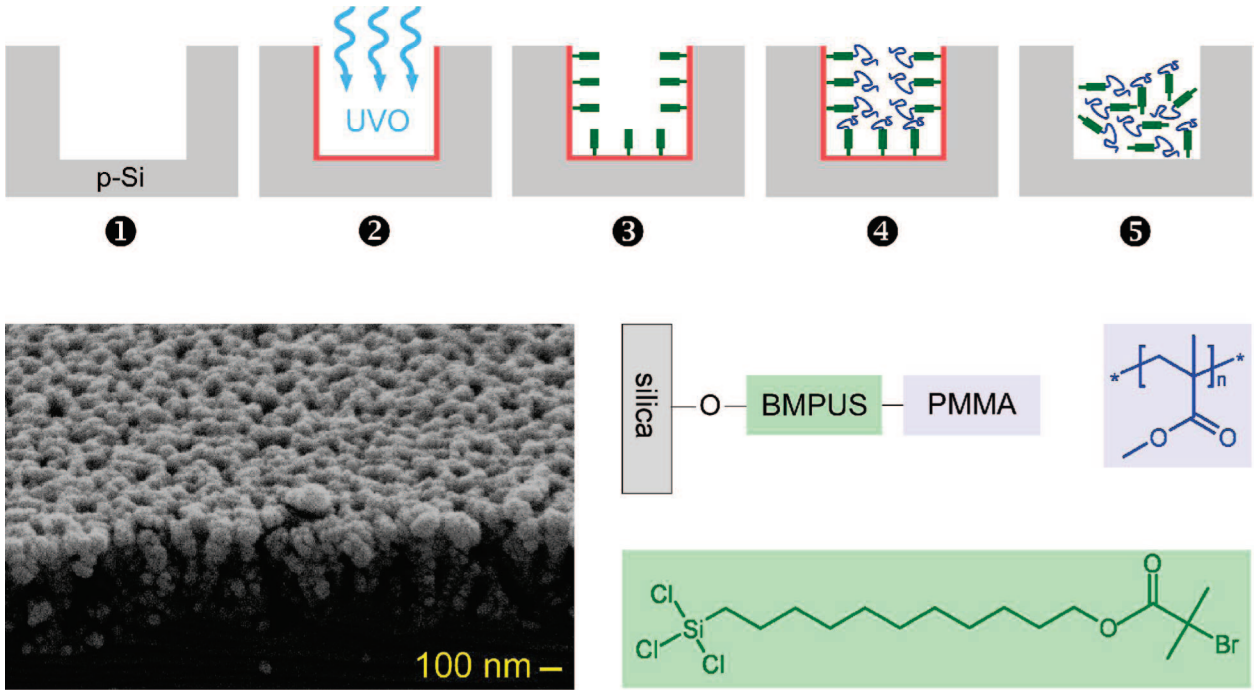

Figure 3. (top) Schematic depicting the steps leading to the formation of grafted PMMA brushes inside porous silicon (p-Si). Porous silicon was made using the procedure described in the text (1). Scanning electron microscopy experiments revealed that the pores have an average size of ≈50 nm, as determined using scanning electron microscopy (bottom left). The specimens were exposed to UVO treatment (2), which created a thin silica layer on the surface of the pore. This silica layer served as an attachment substrate for organosilane-based initiator (BMPUS, shown on bottom right), which was deposited from toluene solution and formed a self-assembled monolayer (3). PMMA chains were grown via surface-initiated polymerization of MMA from the BMPUS centers inside the pores (4). After polymerization, the silica layer was removed by etching the specimens with hydrofluoric acid vapor (5), which removed the silica underlayer and left the polymers inside the pores.

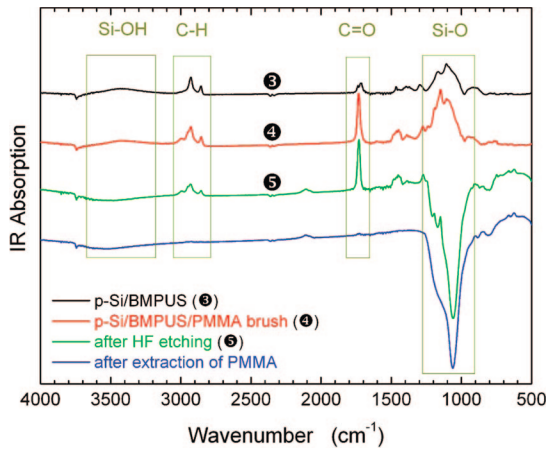

Figure 4. FTIR spectra monitoring the steps involved in preparing PMMA brushes inside p-Si. The various steps are described in the text. The labels correspond to those used in Figure 3.

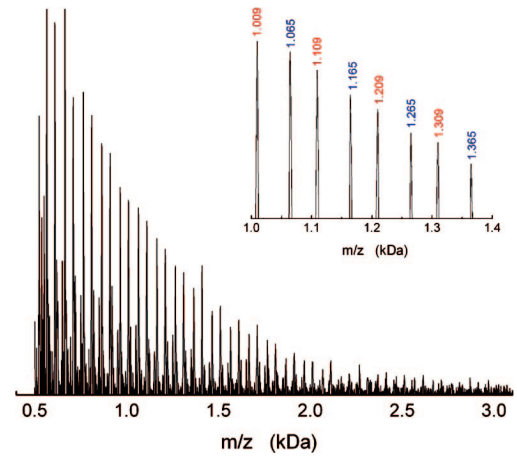

Figure 5. DIOS-MS spectrum from PMMA brush grown inside p-Si for 180 min. The inset depicts two distributions of molecular weights presumably resulting from two different cleavage mechanisms of the polymer from the substrate. Note that the separation between any two peaks in each distribution corresponds to that of a single MMA unit.

technique described earlier. The presence of pore-grown PMMA was indicated by a slight shift and an increase in the relative intensity of the carbonyl stretch at 1732 cm^{-1} (second spectrum from the top in Figure 6). Attempts to liberate the PMMA chains from AAO using HF vapor to cleave the Si−O bonds of the initiator only yielded small amounts of material. Exposing PMMA-containing AAO substrate to concentrated HF solution and subsequent analysis by MALDI-MS gave samples with an observed repeat unit of about 75 Da, which was much lower than the expected 100.1 Da for a neat MMA. Because the ester functionality present in each MMA monomer units is susceptible to hydrolysis in the presence of a strong acid such as HF,[49,50] there is a possibility of hydrolysis taking place when exposed to concentrated HF. This problem was not encountered with the cleavage of the PMMA from the porous silicon with HF vapor (the MMA repeat unit was consistently ≈100.1 Da), presumably because of short exposure times in those experiments. As use of HF vapor was unsuccessful and use of concentrated HF gave possibly hydrolyzed polymer, more dilute HF solutions were explored as means to detach the polymer from the substrate. It was found that treatment with 10% aqueous HF solution provided PMMA in larger amounts than that obtained with HF vapor and with the expected mass of each MMA repeat unit.

After cleaving PMMA from the AAO supports, chloroform was used to separate the surface grown-PMMA from the aqueous HF solution. The chloroform solution containing the

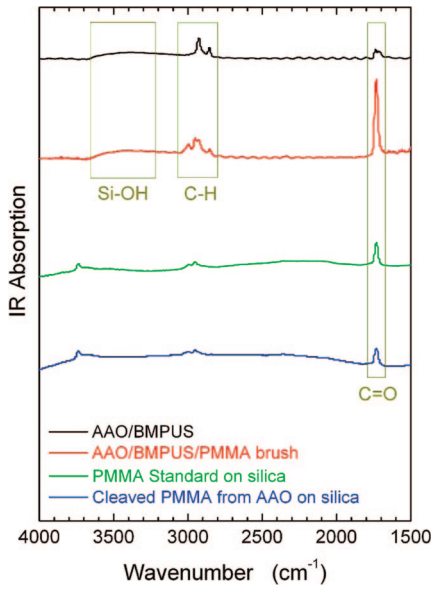

Figure 6. FTIR spectra collected from AAO substrates modified with the BMPUS polymerization initiator (black line) and AAO substrates with PMMA brushes (red line). The blue line represents the FTIR spectrum from PMMA after cleaving from the AAO substrate and placing onto a silicon wafer. Note that this spectrum is identical to that measured on PMMA standard sample (green line) on a silicon wafer.

surface grown-PMMA was extracted, and small drops of polymer-containing solution were placed on an ultraviolet/ozone (UVO)-cleaned silicon wafer. After evaporation of the chloroform, an IR spectrum was taken, which is shown as the bottom spectrum in Figure 6. In order to verify the spectral features in the pore-polymerized PMMA, a 1 mM solution of PMMA standard in chloroform was prepared and deposited as a small drop on a UVO-cleaned silicon wafer. Chloroform was allowed to evaporate, and a transmission IR of the physisorbed PMMA on the silicon wafer was taken. The IR spectrum (second from the bottom in Figure 6) is nearly identical to that of the pore-grown PMMA.

ATRP of PMMA was performed on both BMPUS-modified AAO and in solution using the procedure described in the Materials and Methods section. The polymerization times ranged from 30 to 130 min. After polymerization, the molecular weight distributions of polymers were analyzed with MALDI-MS. Figure 7 shows MALDI-MS spectra for PMMA grown in solution (a, c) and inside AAO pores (b, d) for 30 min (left panel) and 60 min (right panel). The spectra in Figure 7 are normalized, which does not illustrate that the AAO-grown polymers exhibited a lower signal-to-noise ratio than the solution grown polymers because of the much smaller amount of material present. More importantly, inspection of the MALDI-MS spectra reveals stark differences between the molecular weight distributions of the solution- and AAO-grown polymers. For a given polymerization time, the solution polymerization produced polymers with a higher molecular weight relative to the AAO-grown PMMA. Additionally, AAO-polymerized MMA exhibited two different molecular weight distributions that had the same mass of the repeat unit (100.1 Da) but differed likely by the size of the group that has terminated those polymer chains. Following the previous notation, the two distributions are assigned as *84 and *00. In the Discussion section possible chemical structures of the cleaved chains are proposed.

The dependence of $\bar{M}_w$, $\bar{M}_n$, and the polydispersity index (PDI) on polymerization time evaluated using the "point-by-point" analysis for both solution and AAO-grown PMMA is shown in Figure 8. The MALDI-MS data at low molecular weights were hard to resolve because of overlapping MALDI-MS signal from the matrix material. Nevertheless, several other trends could be observed. The molecular weight of the solution grown polymer increased with polymerization time to a value of ≈10 kDa at 120 min. For the AAO-grown polymers, the increase with time was much more modest, reaching a value of only ≈3 kDa in the same time. The polydispersities of the AAO-grown polymers were higher than those of the solution-grown polymer. Finally, comparison of the results in two trials (Figure 8b,c) indicates that the final molecular weights obtained were similar. However, the increase in molecular weight with time in these two trials was different.

Discussion

One of the objectives of this work was to show that the molecular weight of polymers with moderate molecular weights can be determined by using DIOS-MS. Experiments with monodisperse PMMA samples indicated that molecular weight distributions obtained by MALDI-MS and DIOS-MS provide comparable results. These results show that DIOS-MS can be a handy tool for monitoring molecular weight distributions of polymers.

Combining DIOS-MS with a study of polymerization in concave geometries (p-Si substrates) facilitated an exploration of the effect of substrate geometry on substrate-initiated polymerization. For convex substrates with sufficiently high curvature the confinement is not that severe, and as a result, the properties of polymer brushes grown from nanoparticles resemble closely those grown in solution. The effect of substrate geometry becomes more apparent when moving from convex substrates to flat geometries and concave substrates. Indeed, a recent computer simulation study[14] indicated that polymers grown from flat substrates may experience substantial "crowding effect" particularly when growing from substrates having a high areal density of polymerization initiators. Concave geometries should impose the most severe confinement effect among all substrate geometries. Specifically, by increasing the confinement effect, i.e., decreasing the diameter of a pore, the crowding of the chains increases the likelihood of termination and ultimately leads to low molecular weights. In addition, decreasing the pore size may affect the transport of monomer and the catalyst to the growing center, which also lead to decreasing molecular weight of the polymer.

In the current work, polymerization of two types of concave spaces, p-Si and AAO, were examined, which had pore sizes of ≈50 and ≈200 nm, respectively. The polymer weights of PMMA were very small when polymerized inside p-Si and were somewhat higher when grown in the AAO pores. Polymers grown in solution under identical conditions exhibited much higher molecular weights than those grown inside AAO pores (cf. Figure 8). Figure 9 shows some results of our previous work of polymerization on flat substrates to put these results in a broader perspective. Specifically in Figure 9 the dependence of the dry thickness of PMMA on polymerization time obtained corresponds to polymerization of MMA under nearly identical conditions;[51] the data were obtained using a protocol described earlier.[52,53] The only difference was a slight variation of the $[CuCl_2]/[CuCl]$ ratio, which was 0.0150, as supposed to 0.0126 used in this work. The molecular weight of PMMA was deduced from the dry thickness (h) using a previously developed approximate relationship:[54] $\bar{M}_n \approx 1200h$, where h is in nanometers.[55] By comparing the results obtained from the solution-based polymerization with those obtained from polymerization on flat and concave substrates, the following picture emerges. For a given polymerization time, polymers grown in solution had the largest molecular weight. For instance, a 2 h polym-

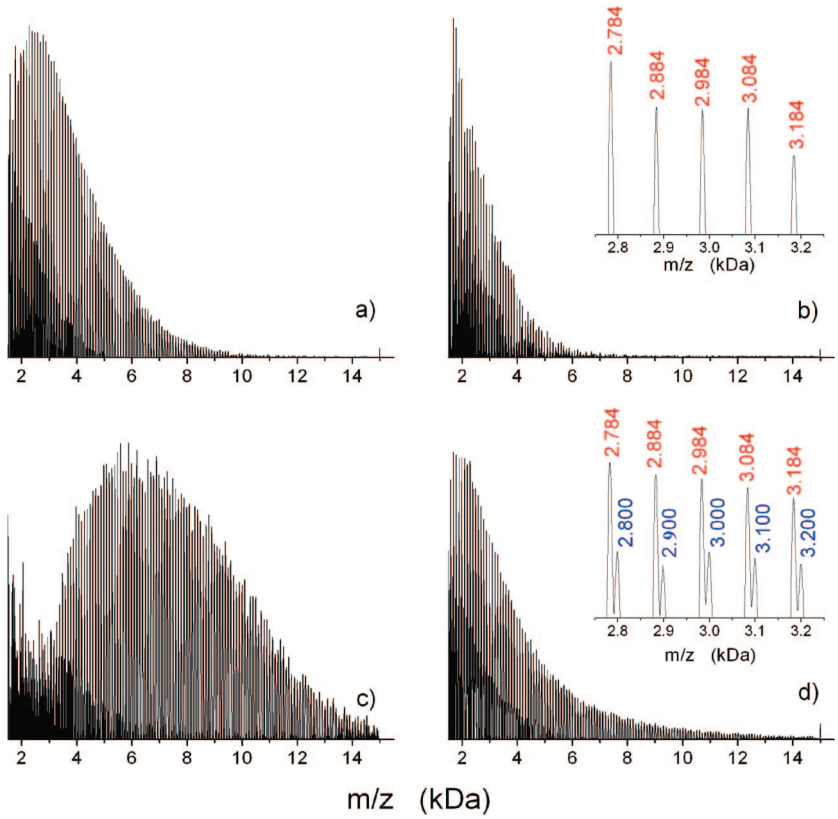

Figure 7. MALDI-MS spectra for PMMA grown in solution (a, c) and inside AAO pores (b, d) for 30 min (a, b) and 60 min (c, d). The insets to (b) and (d) show the the distribution(s) of PMMA with different end groups.

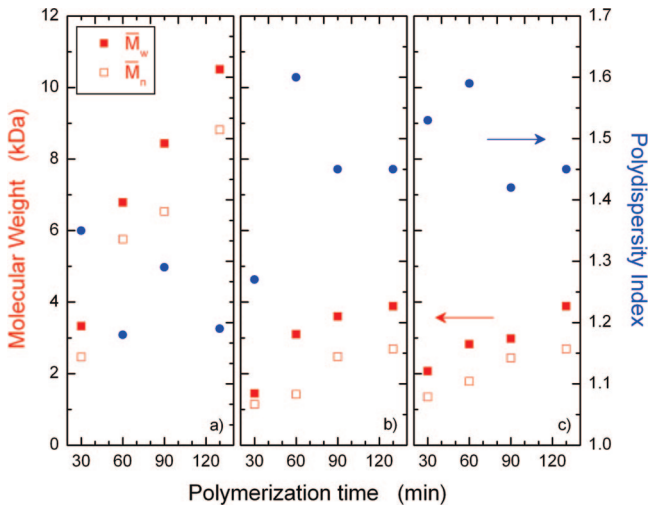

Figure 8. Number-average (open squares) and weight-average (closed squares) molecular weight (left ordinate) and polydispersity (closed circles, right ordinate) as a function of polymerization time for PMMA grown in solution (a) and inside AAO pores (b, c). The molecular weight distributions of the AAO-grown polymers were characterized by a mass of *84 (b) and *00 Da (c).

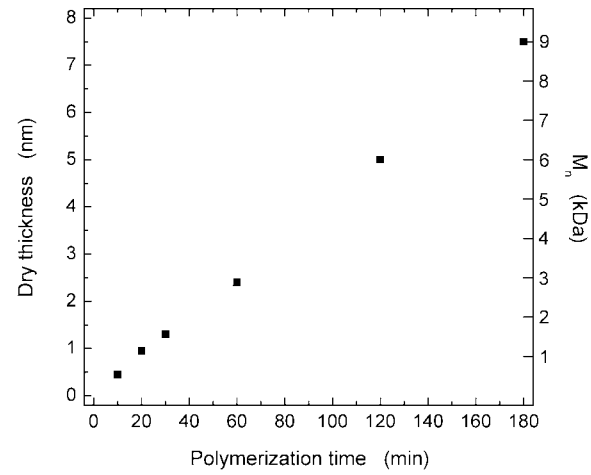

Figure 9. Dry thickness of PMMA brushes grown on a flat substrate under identical conditions as those reported for the concave geometries. The error bars are smaller than the size of the symbol. The molecular weight (in Da) was estimated using an approximate relation $\bar{M}_n \approx 1200h$, where h is dry thickness in nm, developed earlier by Tomlinson and Genzer.[54]

erization of MMA leads to PMMA with $\bar{M}_n \approx 9$ kDa. Introducing confinement decreases the molecular weight of PMMA. While polymerization on flat substrates leads to small decrease in molecular weight, switching to concave geometries imposes strong restrictions on polymerization. For example, while MMA polymerized from flat substrates for 120 min has $\bar{M}_n \approx 6$ kDa, PMMA grown inside 200 nm pores of AAO for the same time have only $\bar{M}_n \approx 3$ kDa. PMMA grown inside p-Si has $\bar{M}_n$ that is smaller than 1 kDa. Clearly, decreasing the size of the pore decreases the molecular weight of the polymers dramatically.

Earlier in this paper it was shown that PMMA cleaved from p-Si and AAO substrates exhibited multiple molecular weight distributions in MALDI-MS and DIOS-MS experiments. Recall that the MALDI-MS and DIOS-MS spectra exhibit peaks with a frequency corresponding to that of the repeat unity of methyl methacrylate (MMA), 100.1 Da. However, these experiments showed several distributions having the same repeat frequency present in the spectra. This can be explained by considering

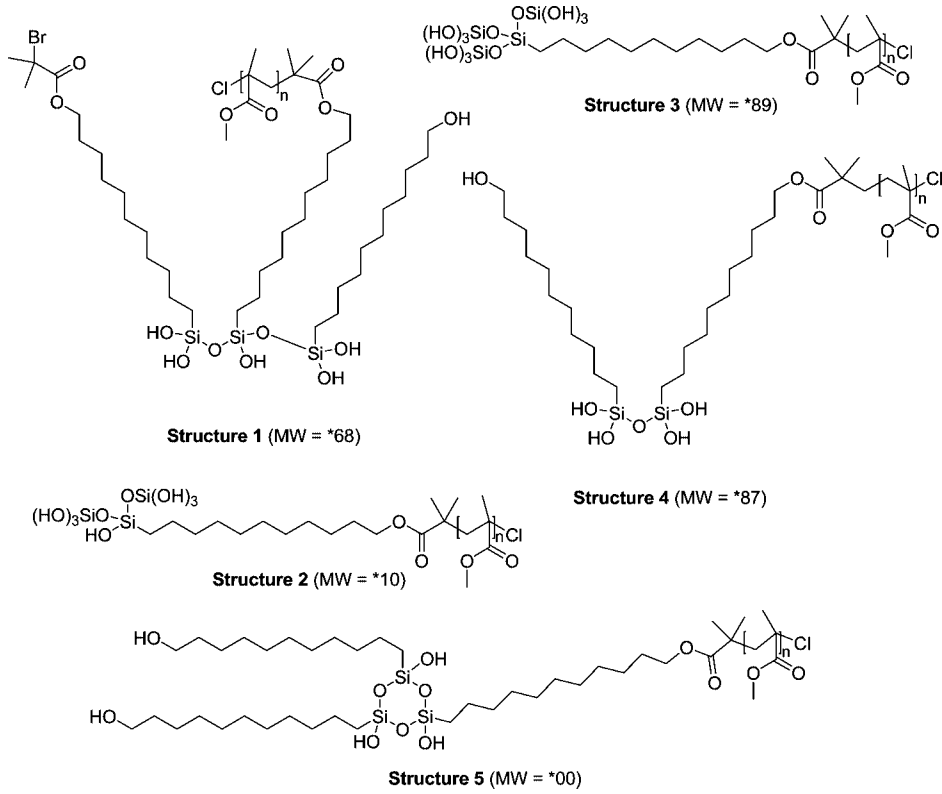

Figure 10. Possible structures that give rise to the molecular weights of PMMA observed with DIOS-MS and MALDI-MS experiments.

that different end groups could be on different populations of molecules. These include different initiator groups (which reflects how the chains cleaved from the substrate) and terminal groups (which reflects how the polymerization terminated). Given the mechanism of ATRP, however, it is proposed that the latter group is likely a tertiary alkyl chloride. This group is considered exclusively in the analysis below. Figure 10 shows five possible end groups that would give rise to the observed molecular weight distributions. Recall that for MMA polymerized in p-Si distributions denoted as *65 and *09 were found. Structures 1 and 2 in Figure 10 possess molecular weights that are close to those detected experimentally via DIOS-MS. AAO-polymerized MMA exhibited distributions denoted earlier as *84 and *00. Those distributions can be approximated by structures 3−5 in Figure 10. To explain the observed molecular weight distributions, in some instances cleavage of the initiator molecule around the ester group and also presence of multiple molecular "bundles" attached to a single cleaved chain were considered. These structures are feasible considering that the efficacy of the initiator is below 100% even for unconfined chains. While these assignments are tenuous at best, the results clearly prove that increasing the curvature of the substrate from flat to concave geometry imposes severe confinement effects on surface-initiated polymerization.

In the analysis presented here, we had to make a few simplifying assumptions. First, in comparing the results of polymerization initiated from concave geometries to those originating from flat substrates, we assumed that the initiator density and efficacy was the same on both substrates. Future work should establish the density of the BMPUS initiators inside the pores and compare it to that on flat substrates. Second, it is assumed that all chains were cleaved off the substrates for the subsequent MS analysis. We justified this assumption by following the procedure with IR spectroscopy, which indicated that within the resolution limit of FTIR no chains were present on the substrates. Third, we assumed that there is no transport limitation associated with delivering monomers to the reaction site inside the pores. This assumption is well-justified as the concentration of monomers was very large, and thus, monomers should be present in large quantities at least close to the entrance of the pores. However, at present we cannot provide solid evidence that there is no constraint on the monomers to enter the pores and participate in polymerization. Finally, we considered that confinement does not influence or alter the ATRP mechanism. At present we cannot comment on the latter issue. In summary, while more work is needed to establish the systematic effect of pore size on the properties of "grafted from" polymers and the limitations listed above, our results provide evidence that increasing the concaveness of the substrate may indeed impose severe limitations to polymers grown from substrates.

Conclusions

The major thrust of this work was to study the effect of concave confinement on polymerization from surfaces. Two porous substrates (i.e., porous silicon (p-Si) and anodic aluminum oxide (AAO) substrates) were studied. These had a nominal pore size of ≈50 and ≈200 nm, respectively. These were used as templates for "grafting from" polymerization of methyl methacrylate (MMA). While MMA polymerized from those two substrates, leading to poly(methyl methacrylate) (PMMA), the molecular weight of the resulting polymer was much lower than that observed in solution-based polymerization of MMA. By comparing the experimental results of polymerization in three different geometries—solution, flat substrate, and concave substrate—it is concluded that these systematically increased the confinement of the growing chains which ultimately lead to a decrease in the molecular weight of the grown polymer.

It has also been demonstrated that DIOS-MS is capable of determining the molecular weight distribution of moderately sized PMMA (up to ca. 6 kDa molecular weight) polymers.

The utilization of DIOS-MS as an analytical tool for establishing the molecular weight distribution of low molecular weight polymers is unprecedented and potentially very useful as it removes the limitations of the "matrix effect" frequently encountered in MALDI-MS experiments.

Acknowledgment. This research was supported by the National Science Foundation and the Petroleum Research Fund under contracts CTS-0403535 and 45688-AC7, respectively, awarded to J.G. C.B.G. thanks the National Science Foundation (CHE-0451120) for funding.

Supporting Information Available: Procedure for deposition of BMPUS initiator and normalized carbon edge data for various monolayer deposition temperatures and times. This material is available free of charge via the Internet at http://pubs.acs.org.

Appendix. Determination of the Number-Average and Weight-Average Molecular Weight from MALDI-MS and DIOS-MS Spectra

In the past, various empirical functions have been introduced to describe experimentally measured molecular weight distributions. One of them, suggested by Schulz, is a two-parameter most probable distribution having a general form

$$w(N) = \frac{(-\ln p)^{k+1} N^k p^N}{\Gamma(k+1)} \quad (1)$$

where p and k are adujstable parameters, N is the degree of polymerization, and Γ is the Gamma function. $\bar{M}_n$ and $\bar{M}_w$ are related to the p and k parameters through the equations

$$\bar{M}_n = -\frac{k}{\ln(p)} \quad (2)$$

$$\bar{M}_w = -\frac{k+1}{\ln(p)} \quad (3)$$

In addition to parameters p and k, a multiplication parameter (A) was used to match the weight fraction $w(N)$ with the experimental data sets.

In addition, eqs 4 and 5 were used to determine $\bar{M}_n$ and $\bar{M}_w$ using the "point-by-point" distribution fit:

$$\bar{M}_n = \frac{1}{\sum_i \frac{w_i}{M_i}} \quad (4)$$

$$\bar{M}_w = \sum w_i M_i \quad (5)$$

where w_i is the weight fraction of the ith component of the distribution having molecular weight of M_i.

The $\bar{M}_w$, $\bar{M}_n$, and PDI were determined from the MALDI-MS data by first localizing the maxima of the intensity for each peak in the MALDI-MS spectra and fitting them to eqs 1–3 (Schultz distribution) and eqs 4 and 5 (point-by-point method). As discussed in the text, two subsequent MALDI-MS peaks were separated by the molecular weight corresponding to a single methyl methacrylate (MMA) repeat unit. The analysis of poly(methyl methacrylate) (PMMA) brushes prepared by grafting from polymerization of MMA on AAO was more challenging. In all samples, we identified multiple overlapping distributions our MALDI-MS spectra. As discussed in detail in the text, these distributions (each of them having the expected resulted from different end groups present in the cleaved PMMA chains) resulted from different cleavage of the PMMA brushes from the AAO substrate. Each of the molecular weight distribution deconvoluted from the overall MALDI-MS spectra was analyzed separately.

References and Notes

(1) Advincula, R. C. *Polymer Brushes: Synthesis, Characterization, Applications*; Wiley-VCH: Weinheim, 2004.
(2) Matyjaszewski, K.; Miller, P. J.; Shukla, N.; Immaraporn, B.; Gelman, A.; Luokala, B. B.; Siclovan, T. M.; Kickelbick, G.; Vallant, T.; Hoffmann, H.; Pakula, T. *Macromolecules* **1999**, *32*, 8716–8724.
(3) Kong, X. X.; Kawai, T.; Abe, J.; Iyoda, T. *Macromolecules* **2001**, *34*, 1837–1844.
(4) Kim, J. B.; Huang, W. X.; Bruening, M. L.; Baker, G. L. *Macromolecules* **2002**, *35*, 5410–5416.
(5) Husemann, M.; Mecerreyes, D.; Hawker, C. J.; Hedrick, J. L.; Shah, R.; Abbott, N. L. *Angew. Chem., Int. Ed.* **1999**, *38*, 647–649.
(6) Shah, R. R.; Merreceyes, D.; Husemann, M.; Rees, I.; Abbott, N. L.; Hawker, C. J.; Hedrick, J. L. *Macromolecules* **2000**, *33*, 597–605.
(7) Jeon, N. L.; Choi, I. S.; Whitesides, G. M.; Kim, N. Y.; Laibinis, P. E.; Harada, Y.; Finnie, K. R.; Girolami, G. S.; Nuzzo, R. G. *Appl. Phys. Lett.* **1999**, *75*, 4201–4203.
(8) Kim, N. Y.; Jeon, N. L.; Choi, I. S.; Takami, S.; Harada, Y.; Finnie, K. R.; Girolami, G. S.; Nuzzo, R. G.; Whitesides, G. M.; Laibinis, P. E. *Macromolecules* **2000**, *33*, 2793–2795.
(9) de Boer, B.; Simon, H. K.; Werts, M. P. L.; van der Vegte, E. W.; Hadziioannou, G. *Macromolecules* **2000**, *33*, 349–356.
(10) Ghosh, P.; Lackowski, W. M.; Crooks, R. M. *Macromolecules* **2001**, *34*, 1230–1236.
(11) Jones, D. M.; Huck, W. T. S. *Adv. Mater.* **2001**, *13*, 1256–1259.
(12) Hyun, J.; Chilkoti, A. *Macromolecules* **2001**, *34*, 5644–5652.
(13) Osborne, V. L.; Jones, D. M.; Huck, W. T. S. *Chem. Commun.* **2002**, 1838–1839.
(14) Genzer, J. *Macromolecules* **2006**, *39*, 7157–7169.
(15) von Werne, T.; Patten, T. E. *J. Am. Chem. Soc.* **1999**, *121*, 7409–7410.
(16) von Werne, T.; Patten, T. E. *J. Am. Chem. Soc.* **2001**, *123*, 7497–7505.
(17) Perruchot, C.; Khan, M. A.; Kamitsi, A.; Armes, S. P.; von Werne, T.; Patten, T. E. *Langmuir* **2001**, *17*, 4479–4481.
(18) Carrot, G.; Diamanti, S.; Manuszak, M.; Charleux, B.; Vairon, I. P. *J. Polym. Sci., Part A: Polym. Chem.* **2001**, *39*, 4294–4301.
(19) Bontempo, D.; Tirelli, N.; Masci, G.; Crescenzi, V.; Hubbell, J. A. *Macromol. Rapid Commun.* **2002**, *23*, 418–422.
(20) Tsujii, Y.; Ejaz, M.; Sato, K.; Goto, A.; Fukuda, T. *Macromolecules* **2001**, *34*, 8872–8878.
(21) Yoon, M. S.; Ahn, K. H.; Cheung, R. W.; Sohn, H.; Link, J. R.; Cunin, F.; Sailor, M. J. *Chem. Commun.* **2003**, 680–681.
(22) Di, J. B.; Sogah, D. Y. *Macromolecules* **2006**, *39*, 5052–5057.
(23) Di, J. B.; Sogah, D. Y. *Macromolecules* **2006**, *39*, 1020–1028.
(24) Zhang, J.; Yang, Y. F.; Zhao, C. Z.; Zhao, H. Y. *J. Polym. Sci., Part A: Polym. Chem.* **2007**, *45*, 5329–5338.
(25) Chen, B.; Evans, J. R. G.; Greenwell, H. C.; Boulet, P.; Coveney, P. V.; Bowden, A. A.; Whiting, A. *Chem. Soc. Rev.* **2008**, *37*, 568–594.
(26) Mittal, V. *J. Colloid Interface Sci.* **2007**, *314*000.
(27) Bruening, M. L.; Miller, M. D.; Balachandra, A. M.; Huang, W. X.; Baker, G. L. *Polym. Prepr.* **2003**, *44*, 467.
(28) Miller, M. D.; Baker, G. L.; Bruening, M. L. *J. Chromatogr. A* **2004**, *1044*, 323–330.
(29) Choi, K. Y.; Han, J. J.; He, B.; Lee, S. B. *J. Am. Chem. Soc.* **2008**, *130*, 3920–3926.
(30) Akgun, B.; Boyes, S. G.; Granville, A. M.; Brittain, W. J.; Foster, M. D. *Polym. Prepr.* **2003**, *44*, 514.
(31) Jones, D. M.; Brown, A. A.; Huck, W. T. S. *Langmuir* **2002**, *18*, 1265–1269.
(32) Liu, Y.; Klep, V.; Luzinov, I. *Polym. Prepr.* **2003**, *44*, 564.
(33) Kim, J. B.; Huang, W. X.; Miller, M. D.; Baker, G. L.; Bruening, M. L. *J. Polym. Sci., Part A: Polym. Chem.* **2003**, *41*, 386–394.
(34) Ando, T.; Kato, M.; Kamigaito, M.; Sawamoto, M. *Macromolecules* **1996**, *29*, 1070–1072.
(35) Matyjaszewski, K.; Patten, T. E.; Xia, J. H. *J. Am. Chem. Soc.* **1997**, *119*, 674–680.
(36) Patten, T. E.; Matyjaszewski, K. *Adv. Mater.* **1998**, *10*, 901, and references therein.
(37) Matyjaszewski, K.; Xia, J. H. *Chem. Rev.* **2001**, *101*, 2921–2990.
(38) Wei, J.; Buriak, J. M.; Siuzdak, G. *Nature (London)* **1999**, *399*, 243–246.
(39) Wu, K. J.; Odom, R. W. *Anal. Chem.* **1998**, *70*, 456a–461a.
(40) Pasch, H.; Gores, F. *Polymer* **1995**, *36*, 1999–2005.
(41) Murgasova, R.; Hercules, D. M. *Int. J. Mass Spectrom.* **2003**, *226*, 151–162.
(42) Shen, Z. X.; Thomas, J. J.; Averbuj, C.; Broo, K. M.; Engelhard, M.; Crowell, J. E.; Finn, M. G.; Siuzdak, G. *Anal. Chem.* **2001**, *73*, 612–619.
(43) Jones, D. M.; Huck, W. T. S. *Adv. Mater.* **2001**, *13*, 1256–1259.
(44) Montaudo, G.; Samperi, F.; Montaudo, M. S. *Progr. Polym. Sci.* **2006**, *31*, 277–357.
(45) Tinsley-Bown, A. M.; Canham, L. T.; Hollings, M.; Anderson, M. H.; Reeves, C. L.; Cox, T. I.; Nicklin, S.; Squirrell, D. J.; Perkins, E.;

Hutchinson, A.; Sailor, M. J.; Wun, A. *Phys. Status Solidi A* **2000**, *182*, 547–553.
(46) Peebles, L. H. *Molecular Weight Distributions in Polymers*; Interscience Publishers: New York, 1971.
(47) Schultz, G. V. *Z. Phys. Chem.* **1939**, *B43*, 25.
(48) Shin, K.; Xiang, H. Q.; Moon, S. I.; Kim, T.; McCarthy, T. J.; Russell, T. P. *Science* **2004**, *306*, 76–76.
(49) Smith, P.; Goulet, L. *J. Polym. Sci., Part B: Polym. Phys.* **1993**, *31*, 327–338.
(50) Wang, Q.; Xu, X. *Sci. China, Ser. B: Chem.* **1991**, *34*, 1409.
(51) Tomlinson, M. R.; Genzer, J. Unpublished work.
(52) Tomlinson, M. R.; Genzer, J. *Macromolecules* **2003**, *36*, 3449–3451.
(53) Tomlinson, M. R.; Efimenko, K.; Genzer, J. *Macromolecules* **2006**, *39*, 9049–9056.
(54) Tomlinson, M. R.; Genzer, J. *Langmuir* **2005**, *21*, 11552–11555.
(55) This approximate relation has been obtained by growing chains simultaneously in bulk and on the surface and determining M via size exclusion chromatography and h via ellipsometry. Although it has been found to be valid for a range of methacrylates and acrylates grown from BMPUS initiator layers deposited under identical conditions, this relationship should be considered as an estimate only because it assumes that chains grown under confinement possess the same rate of polymerization as those polymerized in solution. Nevertheless, this relationship provides a very reasonable estimate for the chain grafting density (σ): $\sigma \approx 0.45$ chains/nm^2.

MA8004857